Check for updates

ADVANCED ENGINEERING MATERIALS

www.aem-journal.com

Electro–Thermo–Mechanical Characterization of Shape Memory Alloy Wires for Actuator and Sensor Applications, Part 2: High-Ambient-Temperature Behavior

Dominik Scholtes, Stefan Seelecke, and Paul Motzki*

The typical phase transformation temperatures of commercially available shape memory alloys (SMA) for actuator applications are in the region of 80–90 °C for austenite finish and around 60 °C for martensite start. That limits the areas of application for SMA actuators, as increased ambient temperatures restrict their functionality. Especially in the industrial and automotive sectors, operational temperatures of 80 °C and higher are commonly required. This article discusses the limits of operation temperatures for commercially available SMA actuator wires. Also, methods to increase this critical temperature limit, at which the SMA actuation strain falls below a certain threshold, are proposed. By means of electrothermal actuation experiments, the influence of the variation of bias loads and an additional training method are investigated. Supported by these results, an exemplary valve actuator system is designed, which exhibits consistent stroke in a wide range of ambient temperatures. All experiments and measurements are conducted on a custom designed test bench with the same commercially available SMA wire. The test bench is in the following used again to evaluate the designed SMA valve actuator.

1. Introduction and Fundamentals

A commonly known limit for the application of shape memory alloys (SMA) wire actuators is the ambient temperature. It is set by the transformation temperatures of the alloy, which lie typically at 80–90 °C. This article covers the investigation of the sensor and actuator characteristics of SMA wires at high ambient temperatures up to 100 °C. The study's goal is to examine the limits of operational temperature for an SMA actuator system and how to push those limits and optimize the actuator and sensor performance. The proposed specific data helps to better tune and design SMA wires for applications, where increased ambient temperatures are of concern.

In the published article "Part 1: The Effects of Training" of this research project, an application-oriented characterization method for SMA actuator wires is discussed.[1] That article is focused on the influence of two fundamental training methods and the influence of different loads on the stroke and resistance behavior of SMA actuator wires made from nickel–titanium (NiTi). The experiments are performed at a constant ambient temperature of 23 °C.

Building on that, the methods and experimental parameters introduced in the previous part are also utilized in the following sections. With this, the research is consistently continued and supplemented. The general idea is to develop a basic understanding and approach of how to design an actuator–sensor system that features an increased range of operational temperature and stable characteristics at high material stress. To achieve this, specific data of resistance, stroke and stress are proposed. The article is written to be comprehensive as a standalone work, with some repetition from the previous articles. Nonetheless, the whole picture with all facets is painted by also taking into account the previous articles on the characterization method[1] and the custom designed test rig.[2]

The basics of thermal SMA actuators are discussed widely in research articles since their discovery.[3–7] A summary of these is already given in "Part 1." However, according to the focus of this research, a brief overview of important fundamentals is discussed here as well.

SMAs are often used in the form of wires, which are commercially available mostly made of binary nickel–titanium (NiTi). The material shows high phase transformation temperatures accompanied by highly hysteretic thermal and mechanical characteristics. NiTi actuator wires are Ti rich and undergo a (quasi-)plastic deformation when a load is applied at room temperature. When the wire is then heated to the phase transformation temperature, it returns to its original geometry. This response

D. Scholtes, S. Seelecke, P. Motzki
Intelligent Materials Systems Lab
Center for Mechatronics and Automation Technology
ZeMA gGmbH, 66121 Saarbrücken, Germany
E-mail: dominik.scholtes@imsl.uni-saarland.de

D. Scholtes, S. Seelecke, P. Motzki
Intelligent Materials Systems Lab
Department of Systems Engineering
Department of Material Science and Engineering
Saarland University
66123 Saarbrücken, Germany

The ORCID identification number(s) for the author(s) of this article can be found under https://doi.org/10.1002/adem.202400432.

DOI: 10.1002/adem.202400432

is called shape memory effect and strains of 5% and more can be fully recovered.[5] It is based on a reversible rearrangement of the material's crystal lattice structure, where a phase transformation from martensite to austenite and vice versa takes place. Characteristic temperatures are austenite start (A_s) and austenite finish (A_f) temperature, as well as martensite start (M_s) and finish (M_f) temperature. They are determined by the strain over temperature diagram under a constant load (typically around 200 MPa), which can be observed in **Figure 1**. These transformation temperatures are crucial to determine the approximate maximum operation temperature for an SMA actuator. Not only a high A_f temperature is required for applications at increased ambient temperatures, but also high M_f, which results in a narrow hysteresis. The transformation temperatures and the width of the temperature hysteresis mostly depend on the alloy composition and grain structure, but they are also influenced by the material stress, according to the Clausius–Clapeyron relation.[4,8]

In technical applications, SMA actuator wires are typically heated either by electrical power via Joule heating or less commonly by a high-temperature fluid in contact with the alloy.[9,10] Because of their high energy density, SMA wires are especially suitable for small and lightweight actuator systems, such as valves, small-sized gripping systems, and optical image stabilization (OIS).[11–13] These applications, especially in the industrial sector, must work under a wide range of ambient temperatures. Examples for possible SMA-driven applications in manufacturing processes are active valves for injection molding, valves for tempered media, and small gripping solutions at soldering stations, to name some.[14] For automotive applications in exterior and interior, operational temperatures typically go up to 80 °C to ensure functionality in all climates and operating states. Even if the expected operation conditions are around room temperature, the functionality of actuation systems is required to be robust. Therefore, a certain safety to ensure functionality at varying ambient conditions must be complied with.

Also, the self-sensing feature of SMA wires is taking up an important role as it makes external position sensors dispensable.[15] This sensing is based on a change of the electrical resistance, which is observed when SMAs undergo

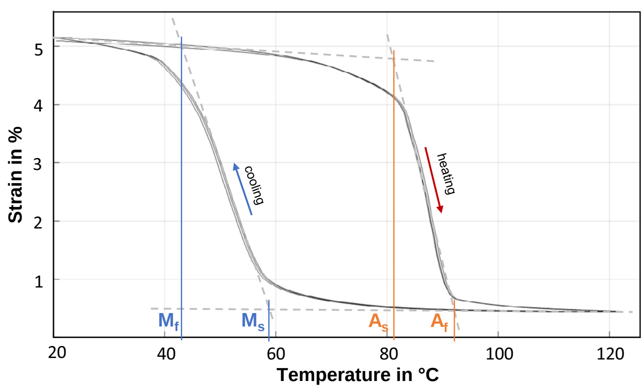

Figure 1. Example of a typical strain versus temperature diagram of a NiTi actuator wire. Depicted are the martensite start (M_s) and martensite finish (M_f) as well as the austenite start (A_s) and austenite finish (A_f) temperatures.

the austenite–martensite transformation or a change in geometry.[16] Their resistance depends on the contemporary crystal lattice, the wire length, and cross-sectional area as well as the temperature.[9,17]

Material characterizations of SMA are usually performed with differential scanning calorimetry, temperature-controlled tensile tests, or thermally induced phase transformation under a constant stress, which is extensively done by Churchill, Iadicola, and Shaw as well as Miller and Lagoudas among others.[6,18–20] Research is also presented on the thermal characteristics of the electrical resistance of NiTi.[21–23] In the field of electrically heated SMA, Lewis et al. investigated the response of Joule-heated wires subjected to convective cooling, while Furst et al. explored the characteristics and self-sensing capabilities of antagonistic Joule-heated NiTi wires.[9,24] The influence of training on the thermal characteristics of NiTi is investigated and the results suggest an increase in transformation temperature by the measure.[25–27] In “Part1” of this research, however, the effects of two fundamental training methods on stroke output and the resistance characteristics of Joule-heated NiTi microwires are examined.[1]

With the learnings from that study, the behavior of SMA actuators under increased ambient temperatures is investigated in this article. The objective of the investigation is the optimization of performance under high ambient temperatures, by combining training and the variation of prestress. The examined thermoelectrical training method promotes consistent material behavior under loads up to 400 MPa. Higher material stress means a higher force output of the actuator, which also leads to a higher work density[28] and suppresses the formation of the R-phase in the NiTi crystal lattice, resulting in a more linear and less hysteretic resistance curve. As existing research based on thermomechanical experiments suggests the additional training is also expected to increase the operational temperature range of SMA actuators.

Due to their rapid cooling rate, small-diameter wires have become important in SMA-driven products like OIS and valve systems.[11,29–31] Consequently, this study is centered on a commercially available NiTi wire measuring 72 μm in diameter. The experimental setup, detailed in another study[2] by Scholtes et al. is purpose built for these microwires. In this article's experiments, two differently conditioned wires are investigated: one conditioned by the manufacturer and another subjected to additional thermoelectrical training.

In the following sections, the impact of training and prestress on the shift of maximum operating temperature of Joule-heated SMA wires is investigated. Based on the results, an exemplary actuator sensor system, which is required to function in a large range of ambient temperatures is conceived and simulated in the test rig. The dynamics of SMA microwires at elevated temperatures is not considered in this study, as it is focused on the effects of load and training on the stroke and resistance characteristics. Future work will be conducted looking into this important field.

The remainder of this article is structured as follows. The experimental setup, the materials and measurement methods, known from the author's prior publications, are described in Section 2. In the subsections of Section 3, the data of the actuation results at temperatures between 23 and 100 °C is presented and discussed for various bias stresses and trained as well as untrained wire samples. Section 4 features the conceptual design and evaluation of a SMA-driven valve suitable for high-ambient temperature operation. The manuscript closes in Section 5 with a conclusion including a summary of the results and an outlook.

2. Experimental Section

The experiments described in the following were carried out using a single setup meticulously detailed by Scholtes et al.[2] For comprehensive information regarding the experiments and test setup beyond the descriptions provided here, please refer to that publication for exhaustive details on design, implementation, and validation.

The custom designed setup, displayed in **Figure 2**, was laid out horizontally. It consisted of two clamps equipped with air bearings that mechanically fixed the SMA wire and established the electrical connections. While one clamp was affixed to a load cell, the other was attached to a linear drive. To avoid any interference from external airflow during measurements, both the clamps and the wire sample were positioned within an isolated chamber. The temperature within the chamber was monitored and could be regulated in a range from 23 to 100 °C.

Additionally, a secondary motor was accessible to install the wire directly from the reel and fixed to the clamps in a stress-controlled regime. This process ensured consistent and repeatable measurement outcomes upon replacing the SMA sample. The test rig was multifunctional, which means that it was designed to conduct tensile tests, actuator tests, and cyclic tests for shakedown experiments or training. The linear drive was run in a closed–loop force–control mode for the actuator tests, where arbitrary loads as well as end stops can be mapped, to simulate real-world applications.

All tests conducted in this article utilized a Joule-heated wire powered by controlled electrical current. The temperature-regulated isolating chamber played a pivotal role in this research, specifically in creating high ambient temperatures. The actuator tests were conducted within this chamber under increased temperatures, applying either a constant load or a linear spring rate alongside a defined prestress.

To facilitate the electrical heating of the SMA wire, a custom-designed constant current source was used, offering adjustable output currents ranging from 0 mA to 250 mA and a voltage of up to 24 V. The precise measurement of the voltage drop across the wire and the electrical current enabled accurate resistance measurement. The setup was controlled using a "National Instruments" FPGA based system and "NI LabVIEW".

For all experiments in this work, a "Dynalloy Flexinol HT" NiTi wire with a measured diameter d_0 of 72 µm (in twinned martensite) was used.[32] The initial wire length L_0 was always set to 100 mm in full austenite at a stress of 10 MPa. This length, set on a virgin wire, was used as the reference value in all experiments. For all following results, the wire strain ε was calculated with

$$\varepsilon = \frac{L - L_0}{L_0} \quad (1)$$

The mechanical stress σ is calculated with

$$\sigma = \frac{F}{A_0} \quad (2)$$

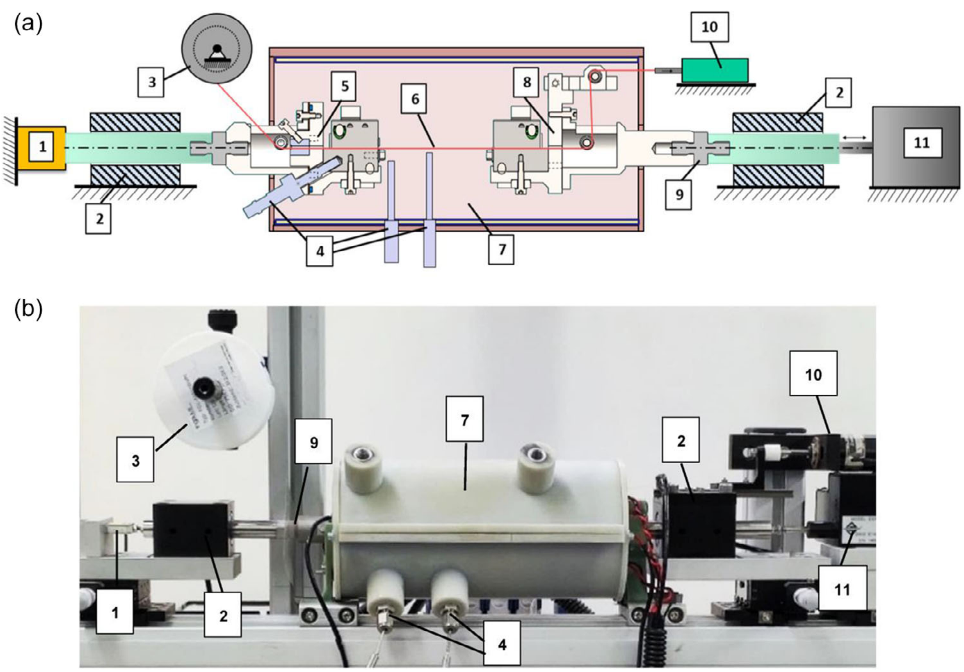

Figure 2. a) Schematic design of the experimental setup. b) Picture of the fully implemented test rig with closed heating chamber including the following components: 1: load cell; 2: air bearing; 3: SMA wire reel; 4: PT100 sensors; 5: fixed wire clamp; 6: SMA wire; 7: heating chamber; 8: moving wire clamp; 9: insulation adapter; 10: prestressing motor; 11: linear direct drive. (Reproduced under terms of the CC-BY license Copyright 2023, Scholtes et al. published by MDPI).[2]

where F is the force acquired by the loadcell and A_0 is the initial cross-sectional area of the wire, which is calculated by

$$A_0 = \frac{\pi}{4} * {d_0}^2 \quad (3)$$

Additionally, a reset procedure was performed on the NiTi wire before each experiment. With this measure, uniform initial conditions for the wire specimen were ensured in every test.

3. Experiments and Results

In "Part 1" of these SMA actuation studies, tensile tests as well as actuator tests are performed, to evaluate the influence of training and different loads on the actuator and sensor properties of NiTi wires. The main learnings are that the wire in the "as-delivered" state is stable up to 200 MPa as intended by the manufacturer and shows good stroke outputs at low stresses. A wide hysteresis in the resistance versus strain signal is observed, indicating the presence of R-phase fractions in the crystal lattice. An additional training with 100 actuation cycles at 400 MPa proved to be superior to the also examined pure mechanical training. It leads to a stable actuator behavior at up to 400 MPa and a decreased resistance–stroke hysteresis. These effects come with the cost of a reduced stroke, a shift in operational range, and a general change in thermomechanical behavior, compared to the as-delivered wire.

The objective is to investigate the actuator and sensor properties at increasing ambient temperatures, pushing the limits for designing temperature stable actuator systems. The focus also lies on optimizing the performance concerning stroke and force in a wide range of operational temperature. Four bias systems relevant for applications are examined. As the continuation of the study in "Part 1", the same load parameters are used. In the following, both samples, untreated and additionally trained, are actuated under a constant stress of 200 MPa as well as a linear bias spring ranging from 100 to 200 MPa. The sample with thermal training is also investigated under 400 MPa constant stress and a spring load of 200–400 MPa. The "as-delivered" wire is not tested under the higher loads, as the previous study already demonstrated its instability and the need for a prior training of the sample.

The range of loads is chosen due to the relevance for applications. Apart from the influence of different stress levels, it also creates a better understanding of how different slopes of the load profiles affect the actuator and sensor performance of the NiTi wire. The prestress of the spring configuration is set at room temperature and is retained at the high-temperature experiments. The expected contraction of the SMA wire due to the ambient condition leads to increased prestresses of the spring, being observed in the high-temperature stress–strain diagrams presented in the following subsections.

The experiments are conducted under temperature conditions ranging from room temperature to 100 in 10 °C steps. When 80 °C is reached and the stroke is less than 1%, the temperature is not increased further. For each test series, only the data of the five highest temperatures is proposed in the following sections. Additionally, the 23 °C experiment, which is also discussed in "Part1," is added as basis for comparisons. For the interpretation and discussion, resistance and stress are displayed over strain for each ambient temperature. The Joule-heated activation of the SMA wire is controlled with a triangular current signal and three repetitions, as displayed in **Figure 3**. With the repetitions, the stability of the behavior can be confirmed, and the possible difference of the first cycle is observable. The triangular current signal offers a varied and continuous input, enabling a thorough examination of the SMA wire's reaction to a spectrum of stimuli compared to, for instance, a square wave. It helps to understand the wire's response under changing current levels, especially concerning stress, strain, and resistance.

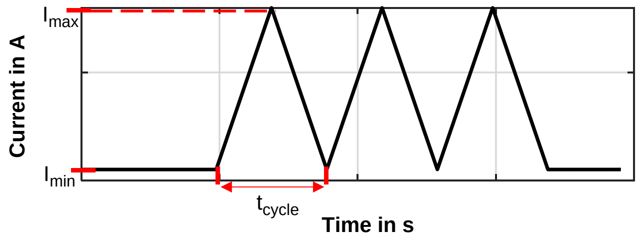

Figure 3. Triangular current input signal for actuation tests with the parameters cycle time t_{cycle}, minimum current I_{min}, and maximum current I_{max}.

Typically for SMA actuators, the first cycle differs from the following cycles due to different starting conditions. In this case, they are caused by the reset test. This reset test is run before each experiment to ensure the same starting conditions for every measurement. For the reset, the wire is slack, heated to full austenite, and then cooled down to ambient conditions with no load applied.

The input parameters of the current signal are cycle time t_{cycle}, minimum current I_{min}, and maximum current I_{max}, as illustrated in Figure 3. The measuring current I_{min} is set to 5 mA for all temperatures, ensuring a consistent resistance measurement. t_{cycle} and I_{max} are adjusted according to the temperature level to guarantee a repeatable and full cooldown of the SMA sample as well as prevent overheating. In **Table 1** the test parameters for the low-stress experiments (100–200 MPa spring load and 200 MPa constant load) are shown. **Table 2** includes the

Table 1. Test parameters depending on the ambient temperature for the low-stress experiments.

Temperature in °C	23	40	50	60	70	80
I_{max} in mA	160	155	140	135	125	120
t_{cycle} in s	40	60	80	80	120	120

Table 2. Test parameters depending on the ambient temperature for the high-stress experiments.

Temperature in °C	23	50	60	70	80	90	100
I_{max} in mA	180	160	155	150	145	140	130
t_{cycle} in s	40	60	80	80	120	120	120

input parameters for the high-stress experiments (200–400 MPa spring load and 400 MPa constant load).

The parameters are identified in preliminary tests. With increasing temperatures, the heating current is reduced to avoid overheating and damaging the NiTi wire. The cycle time is increased accordingly, to ensure a full cooldown at the applied ambient temperature.

3.1. Results of the Untreated Wire Sample under Low Stress

At low material stresses, which in this case means a maximum of 200 MPa, the transformation temperatures are low as well. Thus, a drop in actuator stroke at relatively low ambient temperatures is expected. Using linear springs to bias the SMA wire has the effect that the material stress rises with increasing actuator stroke. Therefore, also the phase transformation temperature of the NiTi wire is not constant but strain dependent.

In **Figure 4**, the results of actuation experiments with a spring prestressed to 100 MPa at 23 °C are displayed for temperatures between 23 and 80 °C. The stress rises to 200 MPa due to the wire's contraction and the spring stiffness. It is observed that with increasing ambient temperature, the minimum strain in austenite stays constant at 0.5%, but the martensitic strain decreases. For an application this means that the initial position cannot be reached after the temperature increases. In a normally closed valve application, for example, the valve would not close properly when a certain ambient temperature is exceeded. Addressing the SMA stroke at significant temperature values, the overall stroke at 23 °C amounts to 4.7%, reduces to 2.2% at 60 °C, and then drops fast to 0.3% at 80 °C.

The resistance curve, displayed in Figure 4 for six different ambient temperatures, shows the typical hysteretic shape evoked by the existence of R-phase portions, which is described in detail in "Part 1."[1] In short, it can be explained by the significant difference in resistivity of the R-phase compared to that of austenite and martensite. As the R-phase only occurs when cooling from austenite to martensite (due to the similarity in lattice structure of R and A), the curves of the heating and cooling path are different.[15,21]

With increasing ambient temperature, the hysteretic behavior remains in place and inner loops of the hysteresis are observed. The slightly lower minimum resistance value of 19.8 Ω for the 23 °C experiment comes from the installation of a new sample for the remaining experiments. With increasing temperature, the minimum resistance values decrease minimally from 20.1 Ω at 40 °C to 20 Ω at 80 °C. Otherwise, the ambient temperature has no significant influence on the resistance characteristics. With increasing temperature, inner loops

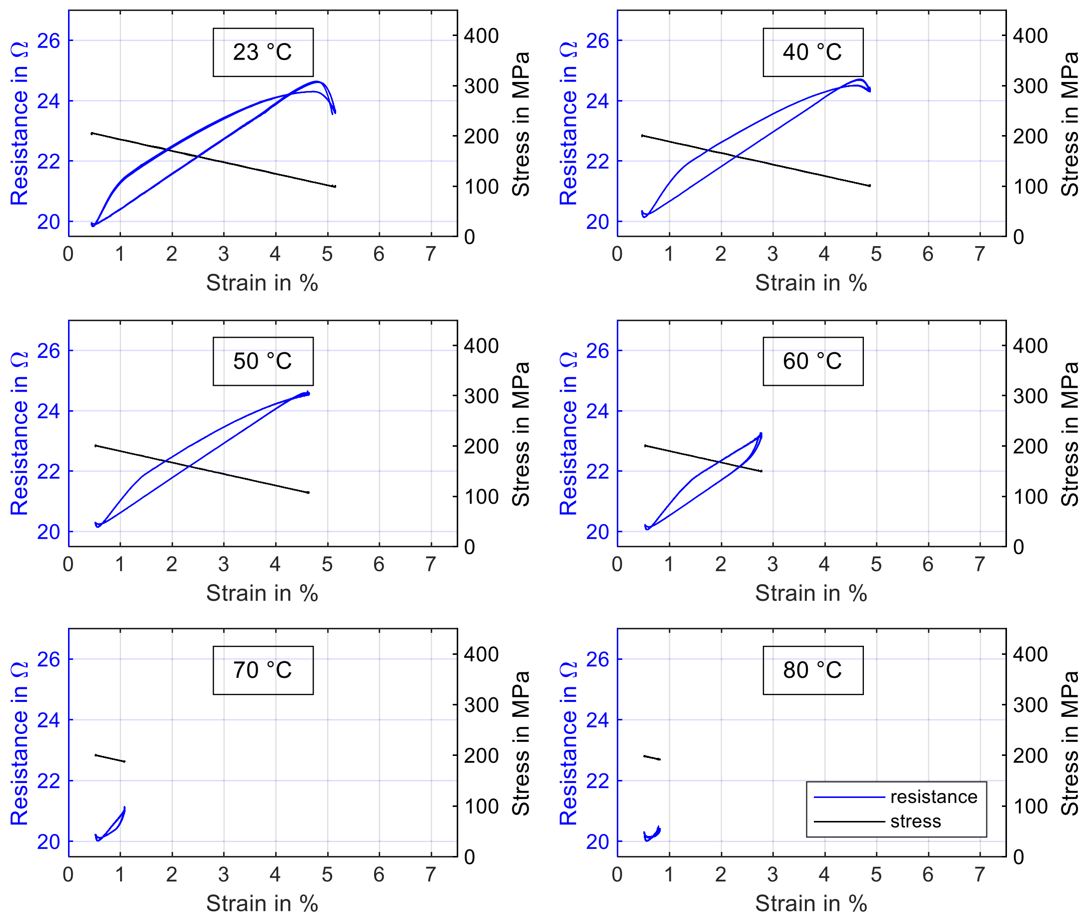

Figure 4. Data of Joule heated actuation experiments with a "Dynalloy Flexinol" NiTi wire of 72 μm diameter under a spring load ranging from 100 MPa (at 23 °C) to 200 MPa at varying ambient temperatures. Displayed are stress and resistance over strain for each temperature.

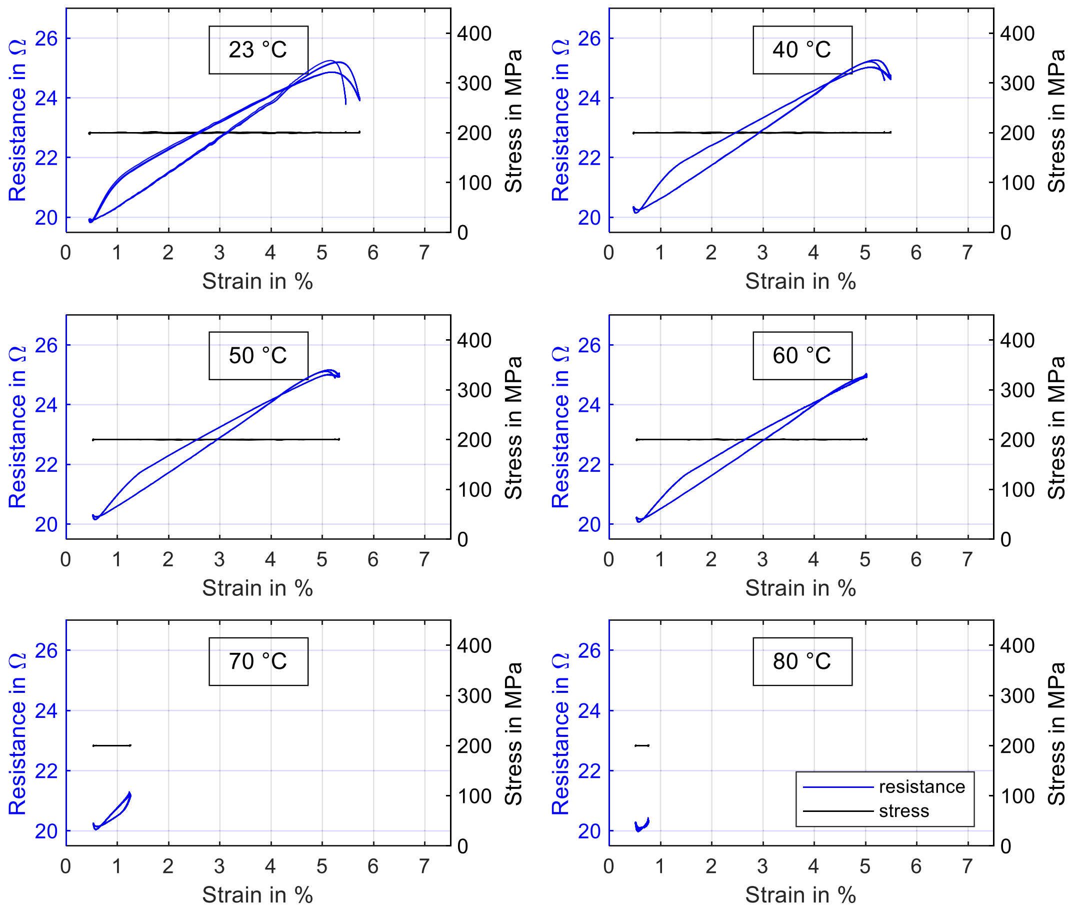

Figure 5. Data of Joule heated actuation experiments with a "Dynalloy Flexinol" NiTi wire of 72 µm diameter under a constant load of 200 MPa at varying ambient temperatures. Displayed are stress and resistance over strain for each temperature.

are formed due to the incomplete retransformation to martensite.

The experimental data of actuator tests with 200 MPa of constant stress are displayed in **Figure 5**. The temperatures of the experiments range from 23 to 80 °C.

Constant loads are less relevant for most technical applications but nonetheless important to understand the influence of the load profile on transformation temperatures. Because of it corresponding to a spring stiffness of zero, the ability to interpolate between the two presented experimental data sets is constituted.

Compared to the spring load, where 200 MPa of stress are applied at full contraction of the actuator only, the material stress is constantly high at all strains and not depending on the wire strain. This leads to increased transformation temperatures of the NiTi, which is most pronounced when looking at the 60 °C results where the stroke ranges at 4.5%. That is a decrease of only 0.8% in relation to the maximum stroke at 23 °C. Compared to that, the low-stress spring load exhibits a stroke of only 2.2% at 60 °C. The stroke then drops more suddenly upon increasing the temperature than with the spring load and ends up at 0.3% at 80 °C. As expected, that is the same value as generated by the spring load with maximum 200 MPa. The resistance hysteresis is, also with the increased overall stress, well pronounced and inner loops are observed with increasing temperature. The width of the hysteresis depends on the material stress, as increased stresses suppress the R-phase. Therefor the width is similar where the stress level of the two experiments is almost equal. At higher strains, the hysteresis of the constant load is reduced compared to the spring load due to the larger stress difference.

Under spring loads, the changing stress influences the transformation temperatures of the material. This leads to a less discrete temperature where the crystal lattice changes configuration. In a strain–temperature diagram, like displayed in Figure 1, this results in less vertical and more angled transformation areas. Due to the constant stress in the data displayed in Figure 5, the material's transformation temperatures are discrete. A rather sudden and more defined drop in actuation strain after exceeding 60 °C is therefore evident.

Combined with the larger overall stroke of the 200 MPa experiment, several lessons can be learnt for SMA-driven applications. When focusing on high stroke outputs and increased operational temperatures, a higher stress leads to larger stroke outputs and better functionality at high ambient temperatures. Accordingly, a spring with low stiffness and high pretension, resembling a constant load, is to be preferred as a biasing mechanism for better functionality at elevated ambient temperatures.

3.2. Results of the Thermally Trained Wire Sample Under Low Stress

The wire sample used in this and the following subsection is thermally trained with 100 cycles under a constant load of 400 MPa, by Joule heating the NiTi wire repeatedly. This procedure and the results are discussed in detail in "Part 1."[1] The goal is to create mechanical stability at increased actuation stresses, benefiting in higher force outputs and increased range of operational temperature of an SMA actuator wire. The training furthermore leads to a shift in working point as well as a reduced maximum stroke of the actuator, apparent when comparing the stress–strain curve in **Figure 6** to the same of Figure 4. Also, it is indicated that the resistance hysteresis is reduced by the treatment. The electrical power versus strain diagrams of "Part 1," which can be compared to temperature–strain diagrams, suggest that the slope between A_s/A_f and M_s/M_f is less steep, and the phase transformation is spread over a wider range of temperature.[1] The results of the low-stress spring load actuation experiments under increased ambient temperatures are displayed in Figure 6. Except for the additional training of the SMA wire, the experimental parameters are identical to those in Section 3.1.

It is observed that the width of the resistance hysteresis is smaller than of the untrained wire. The maximum martensitic length (23 °C) is shifted to 6.1% and the largest stroke is reduced to 4%. These are the accompanying effects of the thermal training, as they are mentioned previously. A significant decrease in stroke when reaching temperatures over 50 °C is evident but less pronounced than with the untreated wire. At 70 °C a stroke of 1.4% is still available and 0.7% are maintained at 80 °C. That means, that although the stroke at low temperatures is reduced due to the training, the effect is turned upside down at higher ambient temperatures, indicating that the goal of the training is met. Therefore, the actuator wire is better suited for high-temperature applications after undergoing thermal training. Additionally, the quality of the sensor signal is improved, due to the smaller resistance hysteresis.

The results for the experiments with 200 MPa of constant stress, similar to Section 3.1, are presented in **Figure 7**. Due to the higher material stress over the larger part of the strain curve, the resistance hysteresis is reduced further, compared to the low-stress spring results.

Most importantly to observe is that, due to the training, the stroke at 70 °C lies at 2.3%. This is contrasted by the as-delivered wire (Figure 5), where less than 1% of stroke is remaining.

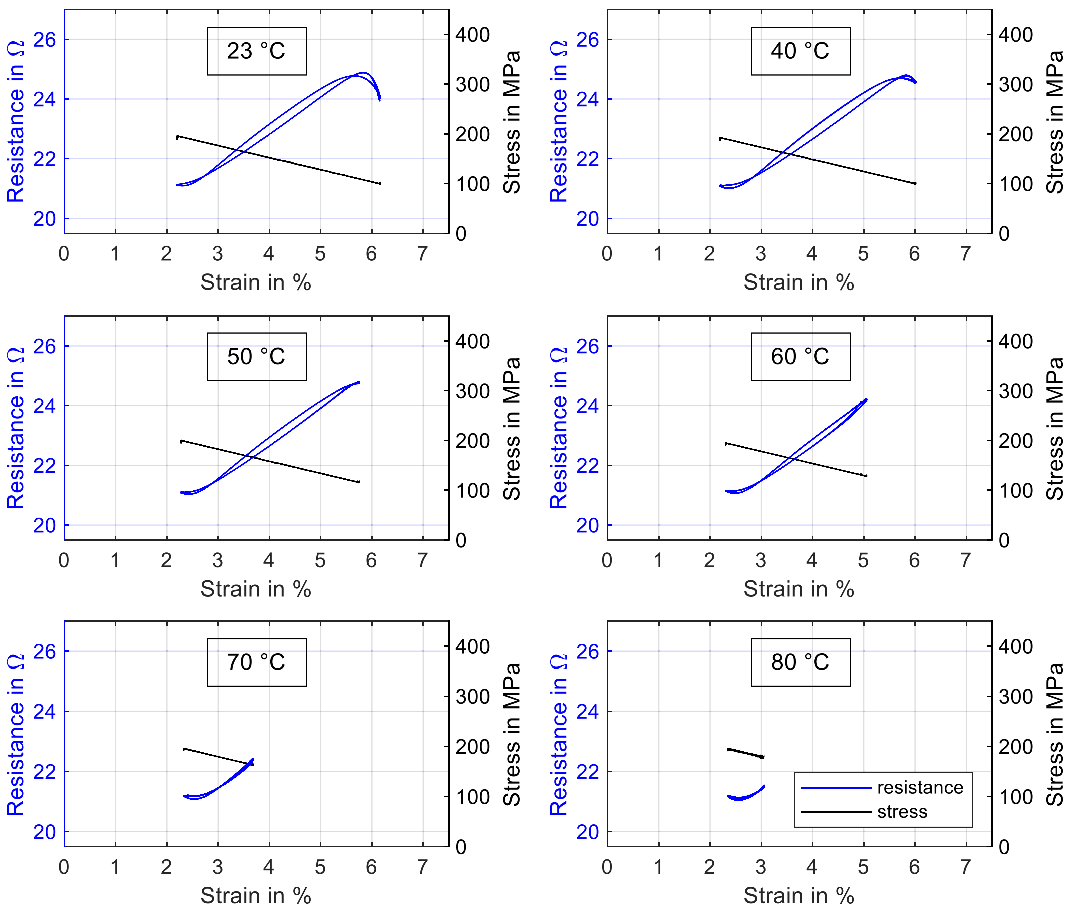

Figure 6. Data of Joule-heated actuation experiments with a "Dynalloy Flexinol" NiTi wire of 72 μm diameter with additional thermal training. It is biased with a spring load ranging from 100 MPa (at 23 °C) to 200 MPa. The experiments are run at varying ambient temperatures. Displayed for each temperature are stress and resistance over strain.

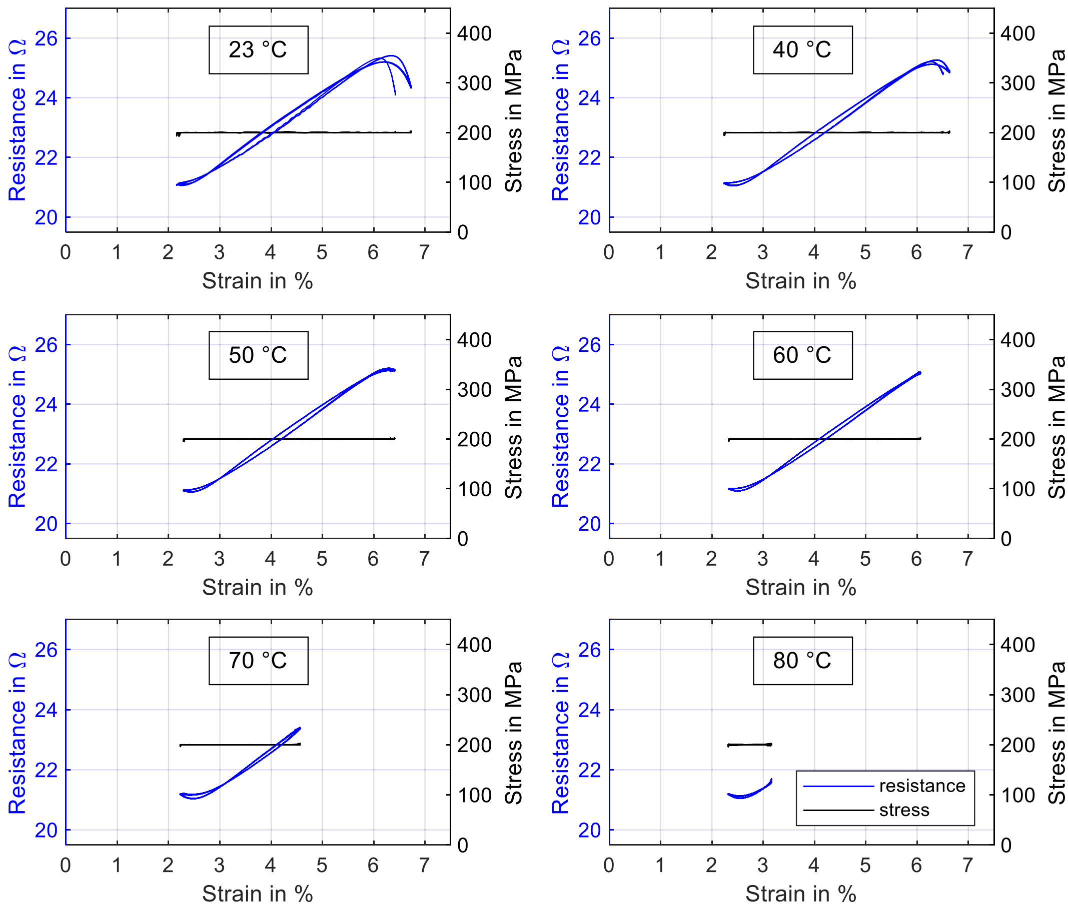

Figure 7. Data of Joule-heated actuation experiments with a "Dynalloy Flexinol" NiTi wire of 72 μm diameter with additional thermal training. It is biased with a constant load of 200 MPa. The experiments are run at varying ambient temperatures. Displayed for each temperature are stress and resistance over strain.

A stroke of over 2% is well utilizable for most application designs and comes with a good fatigue life. However, the threshold of operational temperature where the stroke decreases to slightly under 1% is still under 80 °C.

At this point a first conclusion for low stress actuation at high ambient temperatures can be drawn: The required operational temperatures are an important parameter when designing SMA-driven applications. The results of the discussed experiment for low stresses show that, depending on the stress level and profile, SMA wires in untreated condition feature stroke outputs of 4% and above up to ambient temperatures of 50 to 60 °C. These findings are graphically illustrated in **Figure 8**. It is observed, that under spring load, the phase transformation spreads over a wider range of temperature than the constant load.

Compared to the as-delivered samples, the thermally trained SMA wire exhibits a reduced stroke at low temperatures. At a threshold of about 60 °C, however, the beneficial outcomes of the training become evident. As displayed in Figure 8, the stroke of the trained wire drops less suddenly and a higher stroke at ambient temperatures above about 60 °C is the consequence.

As to be expected due to the Clausius–Clapeyron ratio, a higher stress increases the range of operational temperature. When comparing the spring load to the constant load in Figure 8, the importance of the load profile of the SMA biasing system becomes clear. For applications, a spring with high pre-stress and low stiffness is to be preferred, for reaching high operational temperatures of the actuator system.

The relation of strain to resistance is not shifted by changing ambient temperatures. This indicates a good robustness of the self-sensing against altering ambient conditions.

3.3. Results of the Thermally Trained Wire Sample Under High Stress

Due to the instability of the as-delivered NiTi wire above 200 MPa of material stress, the experiments with 400 MPa and a spring load resulting in 200–400 MPa are only performed with thermally trained wire samples. The results of stress and resistance over strain for the spring load are displayed in **Figure 9**. The maximum ambient temperature for the experiments is increased to 90 °C due to the higher material stress.

The maximum stroke at 23 °C amounts to 4.2%. Up to 70 °C, the stroke output is slightly higher compared to the 200 MPa constant stress experiment, but the difference is not distinctly pronounced. This is caused by the stress increasing only slightly to about 240 MPa at 70 °C.

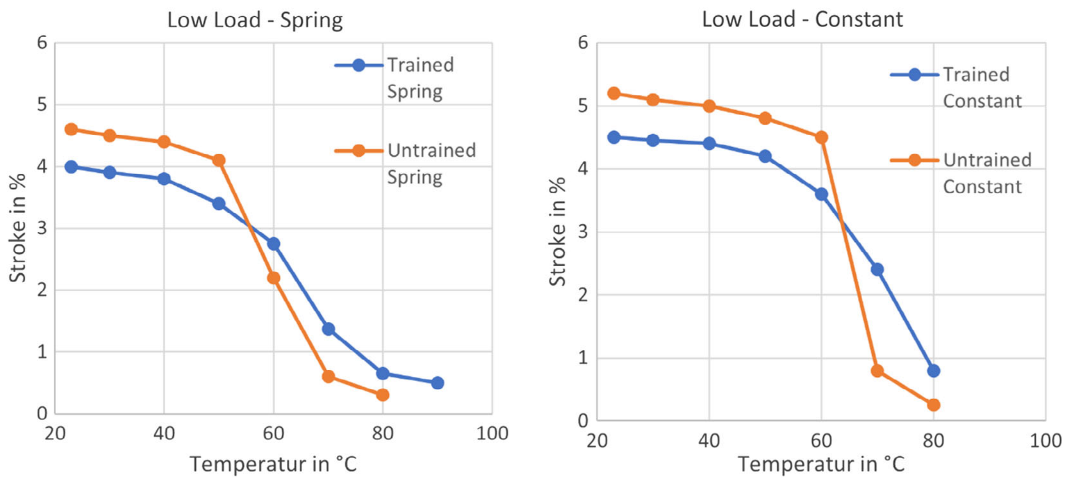

Figure 8. Diagrams of the evolution of the actuation stroke of a 72 µm NiTi wire under increasing ambient temperature. A comparison between the as-delivered wire (orange) and the thermally trained wire sample (blue) is displayed. Left: spring load with maximum 200 and 100 MPa at 23 °C; right: constant load of 200 MPa.

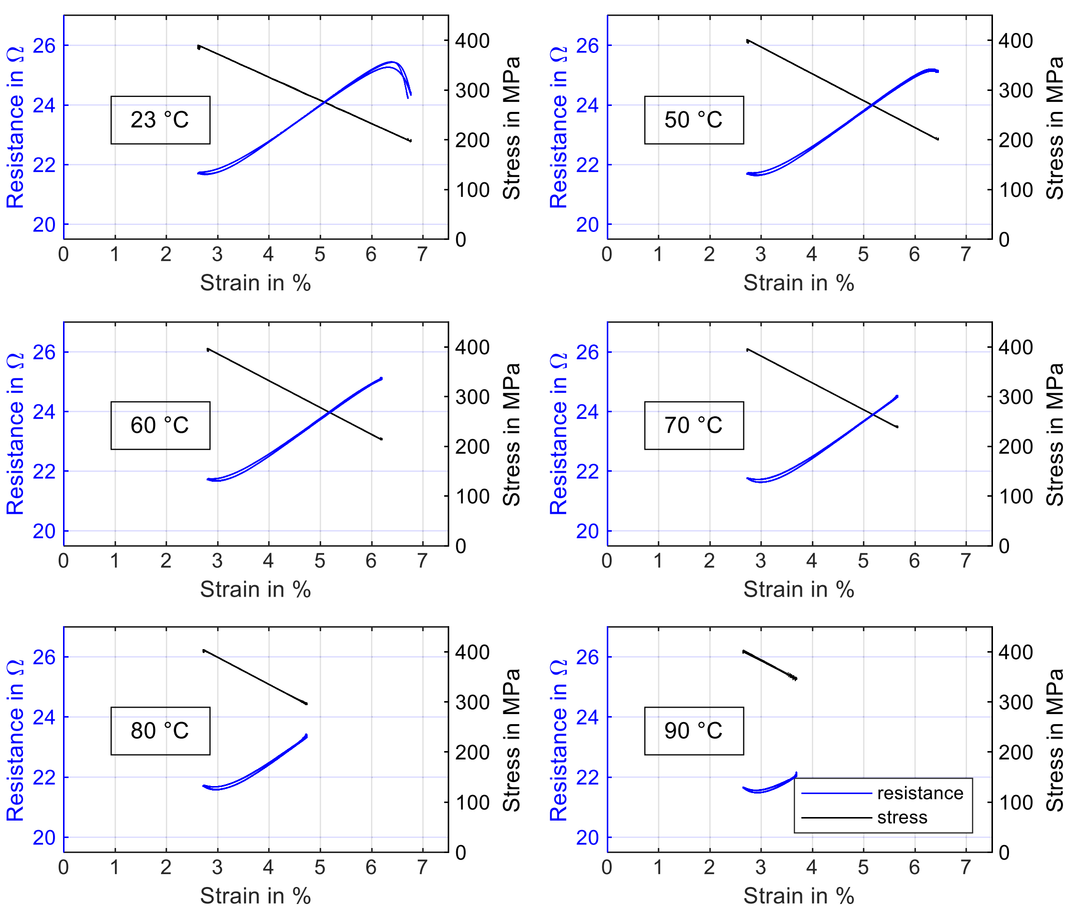

Figure 9. Data of Joule-heated actuation experiments with a "Dynalloy Flexinol" NiTi wire of 72 µm diameter with additional thermal training. It is biased with a spring load ranging from 200 MPa (at 23 °C) to 400 MPa. The experiments are run at varying ambient temperatures. Displayed for each temperature are stress and resistance over strain.

The impact of the higher stress on the resistance hysteresis is however significant. It is reduced to a minimum, resulting from the combination of the training effect and the high stresses suppressing the formation of R-phase portions in the crystal lattice. This effect is independent from the ambient conditions, so that no significant hysteresis is observed in these experiments also at high temperatures.

At 70 °C, an actuator stroke of 2.9% is evident, reducing to 2% at 80 °C. At 90 °C, a strain difference of 1% is measured. Starting at a value of 70 °C, the difference to the 200 MPa constant stress experiment is well pronounced, as the spring rate leads to increasing stress.

From an application perspective it can be derived, that if 2% of strain is set as a minimum requirement for actuator applications, an SMA system with the here-presented parameters can be operated up to 80 °C ambient temperature.

Looking to assess the limits of operational temperatures of SMA wires, the highest overall stress investigated in this research is discussed in the following sections. The resulting data for various ambient temperatures of the actuation experiments with 400 MPa of constant load are presented in **Figure 10**. With such a high stress and the preceding training, it is possible to obtain a working actuator system generating over 2% of stroke at 90 °C. With a maximum stroke of 4.9% at 23 °C, an increase in ambient temperature to 70 °C results in a loss of only 0.5% of stroke, while 4% of stroke can be utilized at 80 °C.

Compared to the data of the high-stress spring load, displayed in Figure 9, the hysteresis in the resistance curve increases slightly due to the higher stress in the beginning of the contraction. A small intersecting loop, with a crossing point in roughly half of the stroke, is observed. This can be explained by the increased influence of temperature, elevating the resistance before the A_s at 400 MPa is reached. The observation underlines the importance of the load profile when targeting a linear and well-interpretable self-sensing signal for a system design.

As expected, the highest load of this investigation exhibits the highest range of operational temperatures. To compare the spring load to the high constant load, the evolution of stroke output over the ambient temperature is shown in **Figure 11**. As shown, the higher overall load results in a larger stroke over the full temperature span. A decisive benefit of the 400 MPa of strain is evident at 80 °C ambient temperature, as the stroke of the spring load amounts to 2%, while the constant load leads to 4% of strain. As already mentioned in the introduction, 80 °C is a crucial value when it comes to applications in the automotive industry for example.

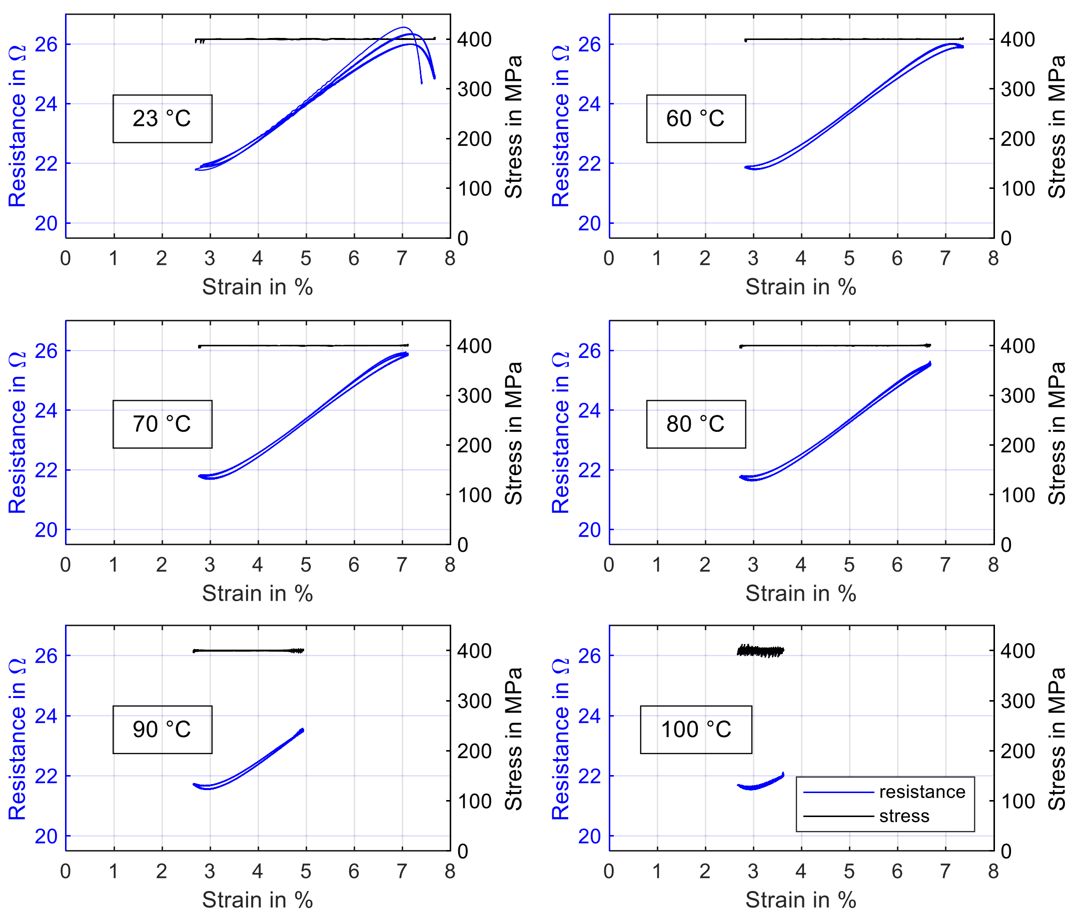

Figure 10. Data of Joule-heated actuation experiments with a "Dynalloy Flexinol" NiTi wire of 72 µm diameter with additional thermal training. It is biased with a constant load of 400 MPa. The experiments are run at varying ambient temperatures. Displayed for each temperature are stress and resistance over strain.

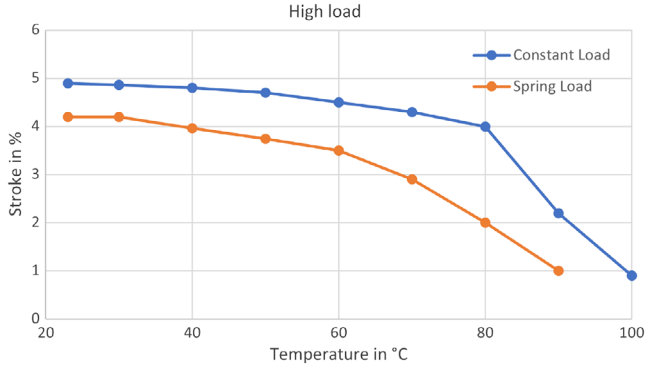

Figure 11. Diagram of the evolution of the actuation stroke of a thermally trained 72 μm NiTi wire under increasing ambient temperature. A comparison between the spring load ranging from 200 to 400 MPa (orange) and the constant load of 400 MPa (blue) is made.

When comparing the results of the high stress in Figure 11 to the evolution of stroke in the low-stress results in Figure 8, the increase in operational range, achieved by thermal training and increased material stress, is obviously recognizable. Although the untrained wire with 200 MPa of constant stress exhibits the largest stroke at room temperature, its performance drops sharply after reaching 60 °C. The 400 MPa constant stress experiments with the additionally trained SMA sample feature almost the same stroke at room temperature but can be run with 4% strain at up to 80 °C. Naturally, increased material stress, alongside with high strains, reduces the lifespan of SMA actuators. Wire stresses of 200 MPa and below are in the region of high-cycle- fatigue life in a Woehler diagram and cycle numbers over 1 million are common.[4,33,34] With stress increased to 400 MPa and strains of 3%, only finite life fatigue is to be expected.[33,34] The strain, on the other hand, also plays an important role in fatigue life of NiTi actuator wires.[4,34] Reducing the wire strain to 1%, for example, and ensuring the stroke by using a longer SMA wire or utilizing transmissions can lead to better fatigue life also under high stresses for operation at increased ambient temperatures. For the application design this means that many parameters must be weighed up against each other to meet the requirements for the task at hand.

4. Application Design for Wide Temperature Range

To showcase the application relevance, the findings and results of the experimental investigation are transferred to an exemplary application concept design. This emphasizes the focus of the research and its relevance for the implementation of SMA-driven systems. As the multifunctional test rig can be used to test SMA microwires against arbitrary loads, the actuator design is tested and validated without having to manufacture a prototype. This makes the evaluation of the SMA system design very fast, as detailed mechanical design and construction are not needed at this early state of a concept phase. The measurements for actuator performance and for the suitability of the resistance signal are precise and meaningful as they are not disturbed by potential problems in the mechanical design of a prototype. As an exemplary application, we choose a small, normally closed valve, with a simple design of an SMA wire working against a bias spring. Valves are a common application for SMA actuators, their detailed design is discussed widely in literature and a variety is already commercially available.[35–37] Britz et al. presented a working prototype of a high-temperature SMA valve.[14]

Under standard conditions, the conceptualized valve works at room temperature, and the pressure p does not exceed 1000 hPa. Under these conditions, the closing time of the valve is to be less than 1 s. Due to the restricted installation space and the necessary stroke of the valve tappet, the required SMA stroke amounts to 3%. The small and lightweight valve has an expected lifetime of 10.000 cycles, which is in the area of finite life fatigue of NiTi at elevated stresses.[33,34,38,39] Although the data of SMA wire manufacturers suggest higher cycle numbers and are supported by first results with high-stress fatigue of SMA actuators, the actuator service life needs to be evaluated in detail inside the actual application.[34,38] The main features of the valve, which are normally closed with SMA opening stroke of 3%, need to stay intact at ambient temperatures of up to 60 °C. At that temperature, the maximum pressure p, against which the valve tappet is required to remain closed, is 250 hPa. For reliable functioning, also after unpredictable events created by environemental influences, a safety factor needs to be taken into account.

A sketch of the valve design is displayed in **Figure 12**. With this sketch, the general functionality of the actuator design in the examplary application is displayed. The normally closed state is enabled by a spring sitting on the valve tappet, which is biasing the SMA wire as well. The movement of the valve tappet is on one end restricted by the valve seat and on the other side by an end stop. The pressurized circular area of the valve tappet has a diameter of 1 mm. Applying the Equation (1) and (2), it becomes evident that the spring force to hold the valve closed against the pressure p corresponds to 200 MPa of material stress of a

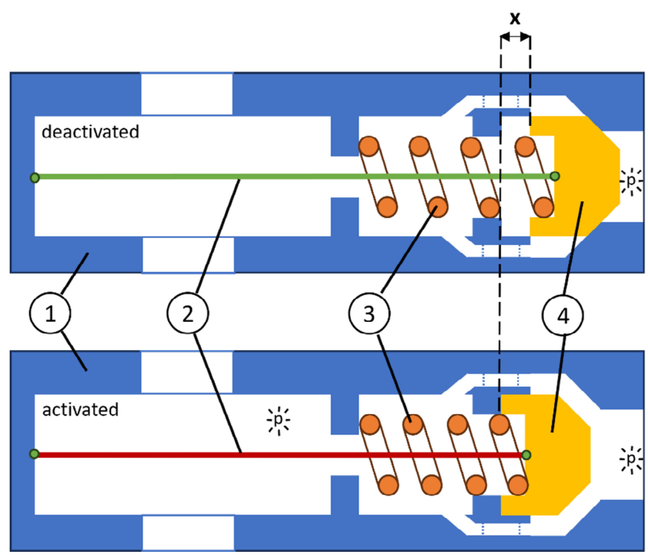

Figure 12. Sketch of the SMA-driven valve in deactivated (upper) and activated (bottom) state. The stroke x between the end stops is marked. The main parts of the design are as follows: 1: valve body; 2: SMA wire; 3: compression spring; 4: valve tappet.

72 µm wire. As by opening the valve, the wire stress increases to over 200 MPa, a thermally trained NiTi wire, as introduced in this study, is used. For reasons of consistency, the already investigated bias spring system ranging from 200 to 400 MPa is utilized. For the actuator test, the two endstops of the design shown in Figure 12 are added at a strain of 6% and 3% to the load profile, resulting in a valve stroke x of 3%. Due to this measure, a constant opening stroke is ensured over a wide temperature range. Design alterations to the valve to manage the flow of fluids, for example, do not influence the working principle of the SMA. However, the dynamics of the SMA wire inside the application are influenced by some additional factors. The forced convection and temperautre of the medium, when in contact to the wire, as well as friction of the valve tappet, can play an important role for example.

The start of transformation reduces the load on the end stop (valve seat), as shown in **Figure 13**, but the valve does not open, due to the high prestress of the spring. Even at a temperature of 60 °C a delta in wire stress ΔF of 50 MPa is resting on the valve seat, as displayed in Figure 13 on the right. That corresponds to a force, high enough to hold the valve closed at 250 hPa of pressure p. With the endstop being positioned at 3% of stain (see Figure 13), the full stroke potential of the SMA wire is not used on purpose. If overloads due to friction or wear result in additional residual strain, the actuator system does not fail immediately thanks to that buffer zone.

The dynamics of the SMA wire will be naturally reduced by the increased ambient temperature. Allthough the activation time is unaffected and could happen in milliseconds, the convective heat transfer to the surrounding air is slower due to the smaller temperature difference. This can be counteracted by active cooling of the SMA wire, submerging the wire in a liquid or choosing an alloy with a higher M_f.[40]

To not electrically overheat the SMA wire in the open position end-stop and take the changing ambient temperatures into account, a feedback control for the Joule heating is needed in such an application. As a feedback, the resistance value of the SMA wire is suitable. In the here-proposed application design, the resistance changes by about 3 Ω between the maximum values. Choosing a fitting algorithm, the end-stops can be detected via the inconsistencies in the evolution of the resistance signal. These inconsistencies are observable in the resistance–strain data of Figure 13 at 3% and 6%, where the endstops are reached.

5. Conclusion and Outlook

In the presented work, the characteristics of Joule-heated SMA microwires at elevated ambient temperatures are investigated. The focus lies on the intricate influence of varying actuator loads combined with additional training on the stroke output and resistance signal. As the second part of a coherent work, the findings from the previous article are developed further and are supplemented.

Various experiments on the as-delivered NiTi wire as well as the thermally trained wire with spring loads and constant loads, each with a low and high stress level, are discussed. The temperature range lies between room temperature and 100 °C. The resulting data implies that increasing the material stress of the SMA actuator from a usual range of 100–200 to 400 MPa raises the operational temperature range about 30 °C. This magnitude is to be expected due to the Clausius–Clapeyron ratio of the material. The additional thermal training, necessary to generate a stable characteristic at elevated material stress, also influences the phase transformation temperature, as existing research also suggests. This reflects on the utilizable stroke at high ambient temperatures as well. Even with low material stresses, the actuator characteristics at 60 °C and above are improved by the measure. However, it is observed that there is a complex relation between training and wire stress, which does not necessarily lead to improved actuator performance. For the examined training process and load parameters, this must be considered when the ambient temperature stays under 60 °C. For the design of actuator sensor systems it needs be taken into account that the fatigue life of SMA actuators is reduced by increasing the wire stress.[41,42] The hysteretic resistance signal also benefits from the training and from the higher actuation stress. The ambient temperature on the other hand does not influence or shift the resistance–strain characteristic. From this it can be concluded that the SMA's self-sensing feature is robust toward altering ambient conditions.

The results are used to conceive an exemplary SMA-driven application, that is then tested by HiL on the multifunctional test rig. A small, normally closed valve, actuated by a 72 µm NiTi wire, is designed. It features a stroke of 3%, working pressures of 250–1000 hPa, and an operational temperature range up to 60 °C.

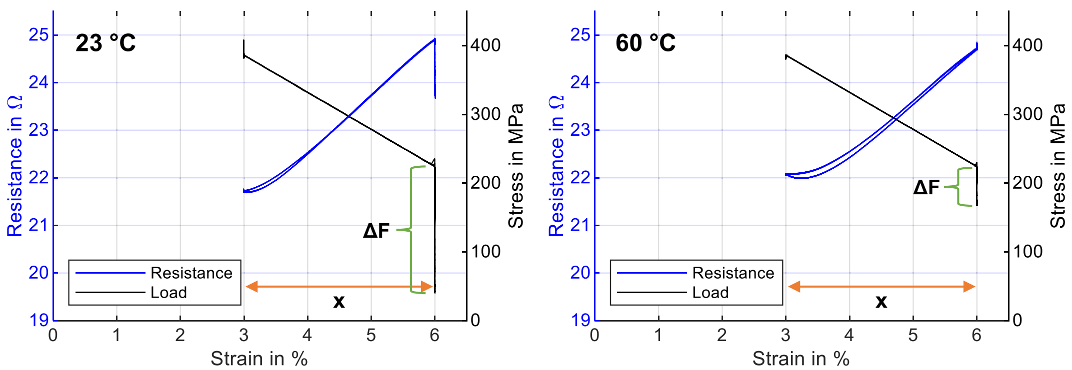

Figure 13. Actuator and sensor characteristics of the SMA wire for the application design. Two distinct operational temperatures are displayed: room temperature on the left and 60 °C on the right.

Next steps to be taken in this field of research are the examination of the dynamics of SMA actuators under high ambient temperatures. Therefore, different excitation waveforms like square waves are utilized for Joule heating to then being able to monitor the cooling time. Furthermore, the influence of other load profiles and stress levels is to be investigated, looking for a sweet spot in stroke utilization. As expected, the cooling time of the SMA increases at elevated ambient temperatures. This behavior can be counteracted by replacing the air surrounding the wire with oil or water.[40] Currently research is being conducted on a specific application with fluid-submerged SMA actuator wires. The same is true for algorithms to compensate the resistance hysteresis and thus read distinct position values from the self-sensing data. Promising high-temperature SMA materials like NiTiHf show the ability to solve many of the issues that come with binary NiTi at high ambient temperatures in the future.[43,44]

Acknowledgements

Open Access funding enabled and organized by Projekt DEAL.

Conflict of Interest

The authors declare no conflict of interest.

Data Availability Statement

The data that support the findings of this study are available from the corresponding author upon reasonable request.

Keywords

ambient conditions, hysteresis, limits, NiTi, resistances, self-sensing, two-way effects

Received: February 19, 2024
Revised: April 9, 2024
Published online: April 23, 2024

[1] D. Scholtes, S. Seelecke, P. Motzki, *Eng. Rep.* **2024**, e12867.
[2] D. Scholtes, M. Schmidt, P. Linnebach, S. Seelecke, P. Motzki, *Materials* **2023**, *16*, 4820.
[3] S. Degeratu, P. Rotaru, G. Manolea, H. O. Manolea, A. Rotaru, *J. Therm. Anal. Calorim.* **2009**, *97*, 695.
[4] L. Fumagalli, F. Butera, A. Coda, *J. Mater. Eng. Perform.* **2009**, *18*, 691.
[5] D. C. Lagoudas, in *Shape Memory Alloys*, vol. *1*, Springer, Boston, MA **2008**.
[6] D. A. Miller, D. C. Lagoudas, *Smart Mater. Struct.* **2000**, *9*, 640.
[7] W. J. Buehler, F. E. Wang, *Ocean Eng.* **1968**, *1*, 105.
[8] C. Velmurugan, V. Senthilkumar, S. Dinesh, D. Arulkirubakaran, *Mater. Today Proc.* **2018**, *5*, 14597.
[9] N. Lewis, A. York, S. Seelecke, *Smart Mater. Struct.* **2013**, *22*, 094012.
[10] C. H. Park, Y. S. Son, SMA spring-based artificial muscle actuated by hot and cool water using faucet-like valve," in Active and Passive Smart Structures and Integrated Systems 2017, SPIE **2017**, 10164T, https://doi.org/10.1117/12.2257467.
[11] Actuator Solutions GmbH, https://www.actuatorsolutions.de/english/products/ (accessed: May 2023).
[12] D. Scholtes, S. Seelecke, G. Rizzello, P. Motzki, in *ASME 2020 Conf. on Smart Materials, Adaptive Structures and Intelligent Systems, SMASIS 2020*, American Society of Mechanical Engineers Digital Collection **2020**.
[13] A. Kazi, M. Honold, W. Rimkus, T. Lokner, M. Bäuml, M. Köpfer, in *ACTUATOR 2018 - 16th Int. Conf. and Exhibition on New Actuators and Drive Systems*, VDE, Bremen **2018**, pp. 375–378.
[14] R. Britz, G. Rizzello, P. Motzki, *Adv. Eng. Mater.* **2022**, *24*, 2200205.
[15] J. J. Zhang, Y. H. Yin, J. Y. Zhu, *Sensors* **2013**, *13*, 12958.
[16] V. Antonucci, G. Faiella, M. Giordano, F. Mennella, L. Nicolais, *Thermochim. Acta* **2007**, *462*, 64.
[17] A. Takimoto, *J. Phys. IV* **1995**, *05*, C8.
[18] C. B. Churchill, J. A. Shaw, M. A. Iadicola, *Exp. Tech.* **2009**, *33*, 51.
[19] J. A. Shaw, C. B. Churchill, M. A. Iadicola, *Exp. Tech.* **2008**, *32*, 55.
[20] C. B. Churchill, J. A. Shaw, M. A. Iadicola, *Exp. Tech.* **2010**, *34*, 63.
[21] F. Gori, D. Carnevale, A. Doro Altan, S. Nicosia, E. Pennestrì, *Int. J. Thermophys.* **2006**, *27*, 866.
[22] C. B. Churchill, J. A. Shaw, *Behav. Mech. Multifunct. Compos. Mater.* **2008**, *6929*, 69291F.
[23] C. B. Churchill, J. A. Shaw, in *Proc. ASME Conf. Smart Mater. Adapt. Struct. Intell. Syst. 2009, SMASIS2009, Oxnard* **2009**, pp. 137–148.
[24] S. J. Furst, J. H. Crews, S. Seelecke, *J. Intell. Mater. Syst. Struct.* **2013**, *24*, 1951.
[25] P. E. Thoma, A. M. Blok, M.-Y. Kao, *MRS Proc.* **1991**, *246*, 321.
[26] D. A. Hebda, S. R. White, *Smart Mater. Struct.* **1995**, *4*, 298.
[27] K. C. Atli, I. Karaman, R. D. Noebe, D. Gaydosh, *Mater. Sci. Eng. A* **2013**, *560*, 653.
[28] W. Kim, B. M. Barnes, J. E. Luntz, D. E. Brei, *J. Mech. Des.* **2011**, *133*, 111010.
[29] S. H. Song, J. Y. Lee, H. Rodrigue, I. S. Choi, Y. J. Kang, S. H. Ahn, *Sci. Rep.* **2016**, *6*, 21118.
[30] Camebridge Mechatronics – Actuators, https://www.cambridgemechatronics.com/en/cml-technology/actuators/ (accessed: August 2023).
[31] S. M. Kirsch, F. Welsch, D. Bevilacqua, D. Naso, S. Seelecke, G. Rizzello, P. Motzki, in *SMASIS 2020 - Conf. on Smart Materials, Adaptive Structures and Intelligent Systems* **2020**.
[32] Dynalloy, http://www.dynalloy.com/pdfs/TCF1140.pdf (accessed: March 2019).
[33] G. Scirè Mammano, E. Dragoni, *Int. J. Fatigue* **2014**, *69*, 71.
[34] SAES Group, https://www.saesgetters.com/sites/default/files/SMARTFLEXSPRINGSANDWIRES.pdf (accessed: July 2018).
[35] A. Czechowicz, S. Langbein, in *Shape Memory Alloy Valves: Basics, Potentials, Design*. Cham: Springer International Publishing, **2015**, https://doi.org/10.1007/978-3-319-19081-5.
[36] M. Tiboni, A. Borboni, M. Mor, D. Pomi, *Proc. Inst. Mech. Eng.* **2011**, *225*, 443.
[37] S. Nalbach, P. Motzki, S. Seelecke, in *ASME 2015 Conf. Smart Mater. Adapt. Struct. Intell. Syst. SMASIS 2015, Coloardo Springs* **2016**.
[38] J. Mayer, P. Molitor, Y. Goergen, P. Motzki, in *Proc. ASME 2022 Conf. Smart Mater. Adapt. Struct. Intell. Syst. SMASIS 2022, Dearborn* **2022**.
[39] G. Scire Mammano, E. Dragoni, *Proc. Eng.* **2011**, *10*, 3692.
[40] A. Pathak, D. Brei, J. Luntz, *Smart Mater. Struct.* **2010**, *19*, 035005.
[41] G. Eggeler, E. Hornbogen, A. Yawny, A. Heckmann, M. Wagner, *Mater. Sci. Eng. A* **2004**, *378*, 24.
[42] D. C. Lagoudas, D. A. Miller, L. Rong, P. K. Kumar, *Smart Mater. Struct.* **2009**, *18*, 085021.
[43] F. Gantz, M. T. Wall, M. L. Young, D. J. Forbes, *Shape Memory Superelasticity* **2022**, *8*, 439.
[44] O. Benafan, G. S. Bigelow, A. Garg, L. G. Wilson, R. B. Rogers, E. J. Young-Dohe, D. F. Johnson, D. A. Scheiman, J. W. Lawson, Z. Wu, *Shape Memory Superelasticity* **2024**, *10*, 55.